Eur. Phys. J. A **27**, 373–380 (2006)
DOI 10.1140/epja/i2006-10009-9

THE EUROPEAN PHYSICAL JOURNAL A

Testing the nature of the Λ(1520)-resonance in proton-induced production

L. Roca[1,a], C. Hanhart[2], E. Oset[3], and U.-G. Meißner[4,2]

[1] Departamento de Física, Universidad de Murcia, E-30100 Murcia, Spain
[2] Institut für Kernphysik (Theorie), Forschungszentrum Jülich, D-52425 Jülich, Germany
[3] Departamento de Física Teórica and IFIC, Centro Mixto Universidad de Valencia-CSIC, Institutos de Investigación de Paterna, Aptdo. 22085, 46071 Valencia, Spain
[4] HISKP (Th), Universität Bonn, Nußallee 14-16, D-53115 Bonn, Germany

Received: 6 February 2006 /
Published online: 3 May 2006 –
Communicated by Xiangdong Ji

Abstract. The $\Lambda(1520)$-resonance has been recently studied in a unitarized coupled-channel formalism with $\pi\Sigma(1385)$, $K\Xi(1530)$, $\bar{K}N$ and $\pi\Sigma$ as constituents blocks. We provide a theoretical study of the predictions of this model in physical observables of the $pp \to pK^+K^-p$ and $pp \to pK^+\pi^0\pi^0\Lambda$ reactions. In particular, we show that the ratio between the $\pi^0\pi^0\Lambda$ and K^-p mass distributions can provide valuable information on the ratio of the couplings of the $\Lambda(1520)$-resonance to $\pi\Sigma(1385)$ and $\bar{K}N$ than the theory predicts. Calculations are done for energies which are accessible in an experimental facility like COSY at Jülich or the developing CSR facility at Lanzhou.

PACS. 14.20.-c Baryons (including antiparticles) – 13.75.-n Hadron-induced low- and intermediate-energy reactions and scattering

1 Introduction

The low-lying negative-parity resonances $J^P = 1/2^-$, $3/2^-$ have recently attracted much attention as many of them can qualify as dynamically generated resonances from the interaction of mesons and baryons. In particular, much progress has been done interpreting the low-lying $1/2^-$ resonances as dynamically generated from the interaction of the octet of pseudoscalar mesons with the octet of stable baryons [1–6] which allows one to make predictions for resonance formation in different reactions [7]. One of the surprises on this issue was the realization that the $\Lambda(1405)$-resonance is actually a superposition of two states, a wide one coupling mostly to $\pi\Sigma$ and a narrow one coupling mostly to $\bar{K}N$ [4,8,9]. The performance of a recent experiment on the $K^-p \to \pi^0\pi^0\Sigma^0$ reaction [10] and comparison with older ones, particularly the $\pi^-p \to K^0\pi\Sigma$ reaction [11], has brought evidence on the existence of these two $\Lambda(1405)$ states [12]. Extension of these works to the interaction of the octet of pseudoscalar mesons with the decuplet of baryons has led to the conclusion that the low-lying $3/2^-$ baryons are mostly dynamically generated objects [13,14]. One of these states is the $\Lambda(1520)$-resonance which was generated from the interaction of the coupled channels $\pi\Sigma(1385)$ and $K\Xi(1530)$. From the experimental point of view this resonance is of particular interest in searches of pentaquarks in photononuclear reactions [15,16] in $\gamma p \to K^+K^-p$ and $\gamma d \to K^+K^-np$. Since getting signals for pentaquarks involves cuts in the spectrum and subtraction of backgrounds, the understanding of the resonance properties and the strength of different reactions in the neighborhood of the peak becomes important in view of a correct interpretation of invariant mass spectra when cuts and background subtractions are made. From the theoretical point of view, in the studies of refs. [13,14], the $\Lambda(1520)$ is build up from the $\pi\Sigma(1385)$ and $K\Xi(1530)$ and couples mostly to the first channel, to the point that, in this picture, the state would qualify as a quasibound $\pi\Sigma^*$ state. Indeed, the nominal mass of the $\Lambda(1520)$ is a few MeV below the average of the $\pi\Sigma^*$ mass. However, the PDG [17] gives a width of 15 MeV for the $\Lambda(1520)$, with branching ratios of 45% into $\bar{K}N$ and 43% into $\pi\Sigma$, and only a small branching ratio of the order of 4% for $\pi\Sigma^*$ which could be of the order of 10% according to some analysis [18] which claims that about 85% of the decay into $\pi\pi\Lambda$ is actually $\pi\Sigma^*$. The association of $\pi\pi\Lambda$ to $\pi\Sigma^*$ in the peak of the $\Lambda(1520)$ is a non-trivial test since one has no phase space for $\pi\Sigma^*$ excitation and only the width of the Σ^* allows

[a] e-mail: luisroca@um.es

for this decay, hence precluding the reconstruction of the Σ^* resonant shape from the $\pi\Lambda$ decay product.

One step forward in the understanding of the $\Lambda(1520)$-resonance has been possible thanks to a recent reaction $K^-p \to \pi^0\pi^0\Lambda$, experimentally performed in ref. [19] and theoretically studied in refs. [20,21]. The reaction proceeds mostly via $K^-p \to \pi^0(\Sigma^{*0}) \to \pi^0(\pi^0\Lambda)$. This is seen at energies of the K^- such that $\sqrt{s} > M_{\pi^0\Sigma^{*0}}$, where the reconstruction of the $\pi^0\Lambda$ invariant mass produces the Σ^{*0} resonance shape [10,20]. However, at energies of the K^- where $\sqrt{s} \simeq M_{\Lambda(1520)}$, the Σ^{*0} is only produced through the tail of the resonance. Yet, a formalism using explicitly the Σ^{*0} propagator allows us to study properly the $K^-p \to \pi^0\pi^0\Lambda$ reaction assuming the same $\pi^0\Sigma^{*0}$ as the dominant mechanism.

On the other hand, the large branching ratios to $\bar{K}N$ and $\pi\Sigma$, of the order of 90% together, indicate that the $\bar{K}N$ and $\pi\Sigma$ channels must play a relevant role in building up the $\Lambda(1520)$-resonance. In the work of refs. [20,21] this problem was tackled by performing a coupled-channel analysis of the $\Lambda(1520)$ data with $\pi\Sigma^*$, $K\Xi^*$, $\bar{K}N$ and $\pi\Sigma$, the first two channels interacting in s-wave and the last two channels in d-wave to match the $3/2^-$ spin and parity of the $\Lambda(1520)$-resonance. In ref. [21] it was also shown that although the $\pi\Sigma^*$ remains with the largest coupling to $\Lambda(1520)$, its strength is reduced with respect to the simpler picture of only $\pi\Sigma^*$ building up the resonance, and at the same time there is a substantial coupling to $\bar{K}N$ and $\pi\Sigma$ which distorts the original $\pi\Sigma^*$ quasibound picture and makes the $\bar{K}N$ and $\pi\Sigma$ channels relevant in the interpretation of different reactions.

In the present work we propose two reactions to test the non-trivial predictions of the unitarized coupled-channel model of ref. [21] regarding the couplings of the $\Lambda(1520)$-resonance to the different channels. These reactions are $pp \to pK^+K^-p$ and $pp \to pK^+\pi^0\pi^0\Lambda$ close to the $\Lambda(1520)$ threshold. Particularly, we show that a measurement of the ratio between the $\pi^0\pi^0\Lambda$ and K^-p mass distributions for $pp \to pK^+\pi^0\pi^0\Lambda$ and $pp \to pK^+K^-p$ reactions, respectively, is an excellent model-independent test of the ratio between the $\Lambda(1520)$ coupling to $\pi\Sigma(1385)$ and to $\bar{K}N$.

The structure of the paper is as follows. In sect. 2 the unitarized coupled-channel model of ref. [21] is summarized. In sect. 3 the dominant mechanism to produce the $\Lambda(1520)$ in p-induced reactions and the implementation of the unitarized coupled-channel model into it is described. Finally, in sect. 4 we show the results for the mass distributions in the two reactions studied.

2 Summary of the unitarized coupled-channel formalism

In ref. [21] the $\Lambda(1520)$-resonance was studied within a coupled-channel formalism including the $\pi\Sigma^*$, $K\Xi^*$ in s-wave and the $\bar{K}N$ and $\pi\Sigma$ in d-waves. Unitarity was implemented by means of the Bethe-Salpeter (BS) equation in the evaluation of the different scattering amplitudes, which reads

$$T = V + VGT \Rightarrow T = [1 - VG]^{-1}V. \quad (1)$$

The kernel of the BS equation is given by the following transition potentials [21]:

$$V = \begin{vmatrix} C_{11}(k_1^0 + k_1^0) & C_{12}(k_1^0 + k_2^0) & \gamma_{13}\, q_3^2 & \gamma_{14}\, q_4^2 \\ C_{21}(k_2^0 + k_1^0) & C_{22}(k_2^0 + k_2^0) & 0 & 0 \\ \gamma_{13}\, q_3^2 & 0 & \gamma_{33}\, q_3^4 & \gamma_{34}\, q_3^2\, q_4^2 \\ \gamma_{14}\, q_4^2 & 0 & \gamma_{34}\, q_3^2\, q_4^2 & \gamma_{44}\, q_4^4 \end{vmatrix}, \quad (2)$$

where the elements 1, 2, 3 and 4 denote $\pi\Sigma^*$, $K\Xi^*$, $\bar{K}N$ and $\pi\Sigma$ channels, respectively. In eq. (2),

$$q_i = \frac{1}{2\sqrt{s}}\sqrt{[s-(M_i+m_i)^2][s-(M_i-m_i)^2]}, \quad (3)$$

$k_i^0 = \frac{s-M_i^2+m_i^2}{2\sqrt{s}}$ and $M_i(m_i)$ is the baryon (meson) mass. The coefficients C_{ij} are $C_{11} = \frac{-1}{f^2}$, $C_{21} = C_{12} = \frac{\sqrt{6}}{4f^2}$ and $C_{22} = \frac{-3}{4f^2}$, where f is $1.15 f_\pi$, with f_π (= 93 MeV) the pion decay constant, which is an average between f_π and f_K as was used in ref. [2] in the related problem of the dynamical generation of the $\Lambda(1405)$. In eq. (1) G stands for a diagonal matrix containing the loop functions involving a baryon and a meson which are regularized by means of two subtraction constants [21]: one for the s-wave channels (a_0) and another one for the d-wave channels (a_2). The treatment of eqs. (1) in refs. [20,21] relies upon a dispersion relation on T^{-1} which allows the on-shell factorization out of the loops of the kernel, V, of the Bethe-Salpeter equation [2,22]. The matrix elements V_{11}, V_{12}, V_{21} and V_{22} come from the lowest-order chiral Lagrangian involving the decuplet of baryons and the octet of pseudoscalar mesons, as discussed in refs. [23,13,14]. The unknown parameters in the V-matrix, as well as the subtraction constants of the loop functions, were obtained by a fit to $\bar{K}N \to \bar{K}N$ and $\bar{K}N \to \pi\Sigma$ partial-wave amplitudes. The values obtained are shown in table 1 [21]. Despite the apparent large number of parameters, it is worth mentioning that the dominant potentials are V_{11}, V_{12}, V_{21} and V_{22} which have no freedom. Let us recall that we do not include $\pi\Sigma^*$ amplitudes in our fit. Hence, the amplitudes involving this channel are genuine predictions of the theory and are shown in fig. 1.

Table 1. Loop subtraction constants and parameters of the potentials. The γ_{13} and γ_{14} are given in units of GeV^{-3} and γ_{33}, γ_{44} and γ_{34} in units of GeV^{-5}.

a_0	a_2	γ_{13}	γ_{14}	γ_{33}	γ_{44}	γ_{34}
−1.8	−8.1	98	110	−1730	−730	−1108

From the scattering amplitudes we can also extract the effective couplings of the $\Lambda(1520)$ to all the different channels, which can be obtained via an analytic continuation of the amplitude in the complex plane. Near the pole we may write up to regular terms

$$T_{ij}(\sqrt{s}) = \frac{g_i g_j}{\sqrt{s} - M_{\Lambda(1520)} + i\Gamma_{\Lambda(1520)}/2} \quad (4)$$

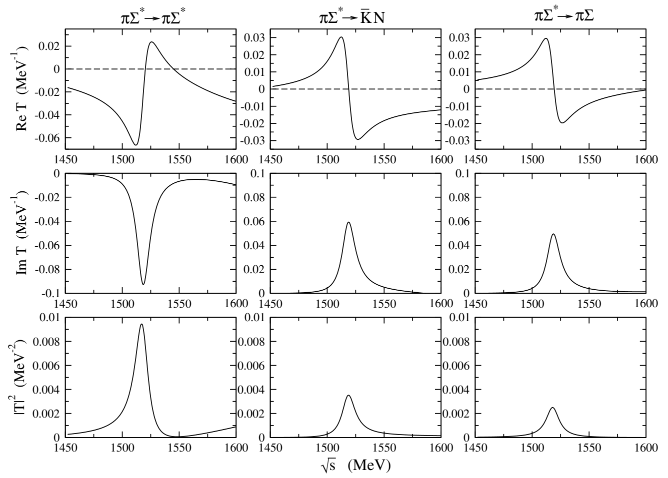

Fig. 1. Unitary amplitudes involving the $\pi\Sigma^*$ channel. From left to right: $\pi\Sigma^* \to \pi\Sigma^*$, $\pi\Sigma^* \to \bar{K}N$ and $\pi\Sigma^* \to \pi\Sigma$.

Table 2. Couplings of the $\Lambda(1520)$-resonance to the different channels.

g_1	g_2	g_3	g_4
0.91	−0.29	−0.54	−0.45

from where we have

$$g_i g_j = -\frac{\Gamma_{\Lambda(1520)}}{2}\frac{|T_{ij}(M_{\Lambda(1520)})|^2}{\mathrm{Im}[T_{ij}(M_{\Lambda(1520)})]}\,, \tag{5}$$

where $M_{\Lambda(1520)}$ is the position of the peak in $|T_{ij}|^2$ and $\Gamma_{\Lambda(1520)} = 15.6\,\mathrm{MeV}$. The couplings obtained are shown in table 2.

3 Proton-induced Λ(1520) production

The amplitudes involving $\pi\Sigma^*$ channels can be investigated in particular in those reactions where this channel plays a significant role. In ref. [21], these amplitudes were checked in the $K^-p \to \Lambda\pi\pi$, $\gamma p \to K^+K^-p$, $\gamma p \to K^+\pi^0\pi^0\Lambda$ and $\pi^-p \to K^0K^-p$ reactions, leading to a good reproduction to the experimental results.

In the present work we apply the model to the $pp \to pK^+(\Lambda(1520)) \to pK^+(\pi^0\pi^0\Lambda)$ and $pp \to pK^+(\Lambda(1520)) \to pK^+(K^-p)$ reactions at energies slightly above the $\Lambda(1520)$ production threshold, which are attainable at a facility like COSY [24,25].

As explained in appendix B, only a single partial wave, with the initial pp pair in the $^1D_2$[1], contributes to the process $pp \to K^+p\Lambda(1520)$ near threshold under the assumption that the $\Lambda(1520)KN$ system in the intermediate state is in an s-wave in all subsystems. In addition, since the production is characterized by a large momentum transfer, we can assume the production operator to be (largely) independent of the final momenta, that are constrained to small values because of the chosen kinematics. Thus the only significant source of an energy or momentum dependence with respect to the final particles should be their various final-state interactions. Therefore, to deduce information on the final-state interactions in large momentum transfer reactions, no detailed knowledge of the production operator is necessary (for a recent review on these issues we refer to ref. [26] and references therein).

There are various ways to derive the relevant matrix elements. The one most commonly used is based on the irreducible tensor techniques and the corresponding formulas are given in appendix B. Here on the main text, on the other hand, we will describe a method for the construction of matrix elements that is more transparent and allows us to easier explain the relevant physics. Needless to say that the final results in the two approaches are identical.

According to the selection rules given above the transition $pp \to \Lambda(1520)Kp$ can be parameterized by a single constant C and a fixed operator structure which reads for non-relativistic final states

$$W = C\left((\mathbf{u}^\dagger_{\Lambda(1520)}\cdot\mathbf{p})(\boldsymbol{\sigma}\cdot\mathbf{p})\sigma_2 u_p^*\right)\phi_K\left(u_p^T\sigma_2 u_p\right), \tag{6}$$

where $\mathbf{u}_\Lambda$ and u_p denote the spinors for the $\Lambda(1520)$ as well as the nucleons. Note, by construction $\boldsymbol{\sigma}\cdot\mathbf{u}_{\Lambda(1520)}$ vanishes. It is this identity that ensures that it is only the pp D-wave that contributes to the above transition operator. For the initial momentum we use $\mathbf{p}$, and $\boldsymbol{\sigma}$ denotes the standard three-vector of Pauli matrices. In the expressions below we will omit the spinors from the initial state to simplify notations.

To come to the corresponding expressions for the full transitions —including the decay of the $\Lambda(1520)$— we need to contract the transition operator W with further operators, namely the spin transition operator $\mathbf{S}$ normalized as

$$\mathbf{S}_i\mathbf{S}_j^\dagger = \frac{1}{3}\left(2\delta_{ij} - i\epsilon_{ijk}\sigma_k\right),$$

as it occurs in the non-relativistic version of the Rarita-Schwinger propagator, as well as the relevant vertices and propagators. As a result for the decay matrix element for the chain

$$pp \to K^+p\Lambda(1520) \to K^+p(\pi^0\Sigma^{*\,0}) \to K^+p(\pi^0[\Lambda\pi^0])$$

we need to replace $\mathbf{u}^\dagger_{\Lambda(1520)\,i}$ in eq. (6) by

$$\Gamma_{\pi\pi} = -\frac{1}{\sqrt{3}}g_1\frac{f_{\Sigma^*\pi\Lambda}}{m_\pi}\bar{u}_\Lambda(p_3)(\mathbf{S}\cdot\mathbf{p}_1)\mathbf{S}_i^\dagger G_{\Lambda^*}(s_{\Lambda^*})G_{\Sigma^*}(s^1_{\Sigma^*}),$$

where we used for the transition $\Lambda(1520) \to \Sigma^*\pi$ a constant matrix element and for $\Sigma^* \to \Lambda\pi$ the standard vertex $\mathbf{S}\cdot\mathbf{p}_1$. In the above expression $-g_1/\sqrt{3}$ is the effective coupling for $\Lambda^* \to \pi^0\Sigma^{*\,0}$ including the isospin factor. Here G_{Λ^*} denotes the propagator of the $\Lambda(1520)$, implicit in the dashed circle in fig. 2, which is a function of $s_{\Lambda^*} = (p_1 + p_2 + p_3)^2$. G_{Σ^*} is the propagator of the Σ^*

[1] Here we use the standard notation for the NN partial waves: $^{2S+1}L_J$, with S, L, J for the total spin, the angular momentum and the total angular momentum.

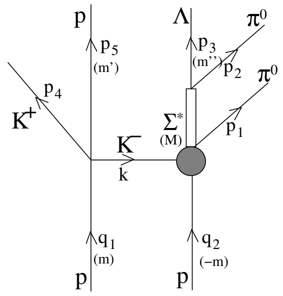

Fig. 2. Mechanism considered for $pp \to pK^+(\Lambda(1520)) \to pK^+(\pi^0\pi^0\Lambda)$.

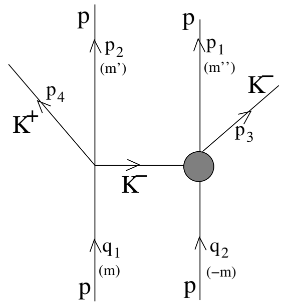

Fig. 3. Mechanism considered for $pp \to pK^+(\Lambda(1520)) \to pK^+(K^-p)$.

being a function of $s^1_{\Sigma^*} = (p_2+p_3)^2$, where we use the standard Flatte parametrization

$$G_{\Sigma^*}(s_{\Sigma^*}) = \frac{1}{\sqrt{s_{\Sigma^*}} - M_{\Sigma^*} + i\Gamma_{\Sigma^*}(\sqrt{s_{\Sigma^*}})/2}\,.$$

Note, to make contact with the T-matrices derived in the previous section we need to replace $g_1 G_{\Lambda^*}$ by the corresponding channel T-matrix. We come back to this below.

After some algebra we get for the complete matrix element in the $\pi\pi\Lambda$ channel

$$\begin{aligned} A^{\pi\pi\Lambda}(p_1,p_2) = &-\frac{Cg_1}{\sqrt{3}}\frac{f_{\Sigma^*\pi\Lambda}}{m_\pi} G_{\Lambda^*}(s_{\Lambda^*})\bar{u}_\Lambda(p_3)\boldsymbol{\sigma}_i\sigma_2 u^*(p_5) \\ &\times \left\{\mathcal{P}(p_1)_i G_{\Sigma^*}(s^1_{\Sigma^*}) + \mathcal{P}(p_2)_i G_{\Sigma^*}(s^2_{\Sigma^*})\right\}, \quad (7)\end{aligned}$$

where $\mathcal{P}(k)_i = (\mathbf{k}\cdot\mathbf{p})p_i - \frac{1}{3}p^2\mathbf{k}_i$ projects on the initial D-wave, as already explained above. One observes that the Λp system in the final state occurs solely in the spin triplet in line with the findings of appendix B.

On the other hand, for the reaction chain

$$pp \to K^+ p\Lambda(1520) \to K^+p(K^-p)$$

we need to replace $\mathbf{u}^\dagger_{\Lambda(1520)\,i}$ in eq. (6) by

$$\Gamma_K = -\frac{1}{\sqrt{2}} g_3 \bar{u}(p_1)(\boldsymbol{\sigma}\cdot\mathbf{p}_3)(\mathbf{S}\cdot\mathbf{p}_3)\mathbf{S}^\dagger_i\,. \qquad (8)$$

We get after some standard manipulations

$$\begin{aligned} A^{Kp}(p_1,p_2) = &-\frac{1}{\sqrt{2}}Cg_3\{\bar{u}(p_1)\sigma_2 u(p_2)(\mathcal{P}(p_3)\cdot p_3) \\ &\times (G_{\Lambda^*}(s_1)+G_{\Lambda^*}(s_2)) \\ &+ i\bar{u}(p_1)\sigma_k\sigma_2 u(p_2)(\mathbf{p}_3\times\mathbf{p})_k(\mathbf{p}_3\cdot\mathbf{p}) \\ &\times (G_{\Lambda^*}(s_1)-G_{\Lambda^*}(s_2))\}\,. \quad (9)\end{aligned}$$

Here the first term contains the two-proton system in a spin singlet state (*e.g.*, $^1S_0$), whereas the second term contains the *pp* system in a spin triplet state. The second term implies $L =$ odd for the two protons. However, as explained in appendix B, the energies of the proton are such that only $L=0$ is relevant. In addition, $G_{\Lambda^*}(s_1) - G_{\Lambda^*}(s_2)$ is much smaller than the sum. Therefore, we will only include the first term in what follows.

As long as we study ratios only, the only unknown in the above expressions, C, drops out and all distributions turn out to be predictions of the model. However, to make contact between the coupled-channel T-matrices of the previous section and the expressions just derived we use a particular production mechanism as shown in figs. 2 and 3. Thus the transition operator parameterized as C contains —in this model— the $KK\bar{N}N$ vertex, where the outgoing K^+ is produced, as well as a $\bar{K}p$ vertex on the other nucleon. We may thus pull the latter out of the definition of C and write

$$-\frac{1}{\sqrt{2}}\tilde{C}g_3 = C.$$

With this definition it is straight forward to show that

$$\tilde{C} = \frac{1}{2f^2}(p^0_4 - k^0)\frac{1}{k^2-m^2_k} \qquad (10)$$

for the transition operator and

$$(g_1)\,G_{\Lambda(1520)}\left(\frac{g_3p^2}{\sqrt{3}}\right) = T_{\bar{K}N\to\pi\Sigma^*}, \qquad (11)$$

$$\left(\frac{g_3p_3^2}{\sqrt{3}}\right)G_{\Lambda(1520)}\left(\frac{g_3p^2}{\sqrt{3}}\right) = T_{\bar{K}N\to\bar{K}N} \qquad (12)$$

for the meson-baryon T-matrices. This completes the evaluation of the production matrix elements.

By the described method the antisymmetrization of the two-proton states has already been taken into account since only allowed partial wave were considered. The symmetrization of the two identical π^0 has to be considered by adding the contribution obtained by changing $p_1 \leftrightarrow p_2$ (see details in appendix B). Hence, $|Amp|^2$ to be used in the cross-section (c.f. eq. (A.2) in the appendix) is given by

$$|Amp|^2 = \sum_{S_z}|A^{\pi\pi\Lambda}(p_1,p_2) + A^{\pi\pi\Lambda}(p_2,p_1)|^2\,. \qquad (13)$$

For the calculation of the cross-sections one has to evaluate a four- and five-body phase space. The method we used is given in detail in appendix A.

Since we have two baryons in the final state which are different for each reaction, the different modification of the cross-section due to the final-state interaction (FSI) of the

ΛN or pp subsystem can be relevant. We have taken this into account by means of the ordinary factor, equivalent to the inverse of the Jost function[2]. For the Λp interaction we use [29] for the factor that multiplies $|T|^2$ in the phase space

$$|C_{FSI}|^2 = \frac{q^2+\beta^2}{q^2+\alpha^2} \tag{14}$$

with

$$\alpha = (1-\sqrt{1-2r/a})/r, \beta = (1+\sqrt{1-2r/a})/r \tag{15}$$

and q the Λ momentum in the $p\Lambda$ rest frame. In eq. (15), a and r are the scattering length and effective range of the s-wave Λp amplitude in $S=1$ which is the state we have. In the calculations we use $a=(-1.4\pm 0.5)$ fm and $r=(4\pm 1)$ fm and we shall estimate the uncertainties induced from these errors.

For the pp final-state interaction in the $pp \to pK^+K^-p$ reaction we use the same expression but with $a=-7.8$ fm (which already accounts for interference with the Coulomb force [30]) and $r=2.79$ fm with significant smaller errors than in the Λp case. This simple prescription is accurate to better than 10% in the region of energies relevant here [31] compared to more elaborate formulas as, *e.g.*, the one given in ref. [32] and is therefore sufficiently accurate for our purposes.

4 Results

First we show in fig. 4 the results for the $\pi^0\pi^0\Lambda$ invariant mass distribution of the $pp \to pK^+\pi^0\pi^0\Lambda$ reaction and the K^-p mass distribution for the $pp \to pK^+K^-p$ (dashed and solid lines, respectively) for an incident proton momentum of 3.7 GeV which is the highest available at COSY. This is also the nominal energy for protons of the developing CSR facility at Lanzhou (China). The different shapes below the peak for the two reactions can be understood from the presence of the Σ^* propagator in the $pp \to pK^+\pi^0\pi^0\Lambda$ reaction, since only its quickly decreasing tail enters in the evaluation of the matrix element.

Although the production rates with this model are of the order of experimental cross-sections measured in the $pp \to ppK^+K^-$ reaction [25], other mechanisms can be at play. In addition, we did not include the initial-state interaction that is expected to lead to a sizable reduction of the cross-section [33], but would not modify the ratio of cross-sections. Because of this we focus on the shape and relative magnitude of our results that are model independent as explained above. In an analogous way to what was studied in ref. [21] for the photoproduction case, we propose to measure the ratio between the $\pi^0\pi^0\Lambda$ and K^-p mass distributions of the $pp \to pK^+\pi^0\pi^0\Lambda$ and $pp \to pK^+K^-p$ reactions, respectively,

$$R \equiv \frac{\mathrm{d}\sigma_{pp\to pK^+\pi^0\pi^0\Lambda}/\mathrm{d}M_{\pi^0\pi^0\Lambda}}{\mathrm{d}\sigma_{pp\to pK^+K^-p}/\mathrm{d}M_{K^-p}}\,. \tag{16}$$

[2] Although the Jost function should not be used for the extraction of scattering parameters from production reactions [27], it still gives, for our case, a sufficiently accurate parametrization for the effect of the final-state interaction [28].

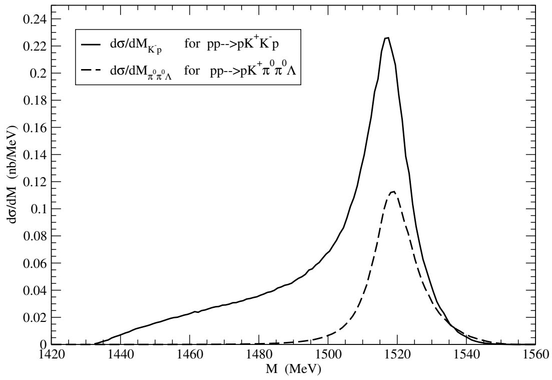

Fig. 4. Solid line: K^-p invariant mass distribution for the $pp \to pK^+K^-p$ reaction. Dashed line: $\pi^0\pi^0\Lambda$ invariant mass distribution of the $pp \to pK^+\pi^0\pi^0\Lambda$ reaction. Incident proton momentum: 3.7 GeV.

Up to phase space, FSI and known numerical factors, the ratio R is proportional to $(|T_{\pi\Sigma^*\to\pi\Sigma^*}|/|T_{\pi\Sigma^*\to\bar{K}N}|)^2$ which, at the $\Lambda(1520)$ peak position, is $(g_1/g_3)^2 = 2.8$ (see eq. (4)). With the full model, the value obtained for R at the peak position is

$$R \sim 0.5 \pm 0.2. \tag{17}$$

The uncertainty given comes from the errors of a and r in eq. (15) when considering the FSI of the final baryons, which is the largest source of uncertainty in our model. Had we not considered the FSI we would have obtained $R\sim 0.9$. Actually, the effect of the FSI is to increase by a factor of ~ 3.6 the K^-p mass distribution and a factor ~ 2 the $\pi^0\pi^0\Lambda$ mass distribution at the peak in the $pp \to pK^+K^-p$ and $pp \to pK^+\pi^0\pi^0\Lambda$ reactions, respectively. These factors emerging from the final-state interactions are strongly dependent on the beam energy.

An experimental measure of this ratio R would provide a good test of the unitarized coupled-channel model since the value of g_1 and g_3 are non-trivial genuine predictions of this theory. Note that the close connection between the nature of a resonance and its effective couplings to the decay channels was derived already in ref. [34] for bound states and extended to inelastic resonances in ref. [35].

5 Summary

We have studied some of the consequences and predictions of a unitarized coupled-channel approach to the $\Lambda(1520)$-resonance through the $pp \to pK^+K^-p$ and $pp \to pK^+\pi^0\pi^0\Lambda$ reactions. The model relies upon a coupled-channel formalism implementing unitarity through the Bethe-Salpeter equation by means of which the resonance structure appears naturally. One of the genuine predictions of this theory are the values of the effective couplings of the $\Lambda(1520)$-resonance to the relevant channels. We propose that the ratio between the $\pi^0\pi^0\Lambda$ and K^-p mass distributions for the $pp \to pK^+\pi^0\pi^0\Lambda$ and $pp \to pK^+K^-p$ reactions, respectively, can provide a test of the ratio between the coupling of the $\Lambda(1520)$-resonance to the

$\pi\Sigma(1385)$ and to $\bar{K}N$ channels. Such a ratio would help to unravel the nature of the $\Lambda(1520)$ and its coupling to meson-baryon components.

We thank A. Sibirtsev for useful comments. This work is partly supported by DGICYT contract number BFM2003-00856, and the E.U. EURIDICE network contract no. HPRN-CT-2002-00311 and the Deutsche Forschungsgemeinschaft through funds provided to the SFB/TR 16 "Subnuclear Structure of Matter". This research is part of the EU Integrated Infrastructure Initiative Hadron Physics Project under contract number RII3-CT-2004-506078.

Appendix A. Five- and four-body phase space

Here we explain in detail the steps followed to simplify the integrals of the phase space in the evaluation of the cross section for the

$$p(q_1)p(q_2) \to p(p_5)K^+(p_4)\pi^0(p_1)\pi^0(p_2)\Lambda(p_3) \qquad \text{(A.1)}$$

reaction (see fig. 2 for the detailed definition of the momenta) with masses M_1, M_2, m_5, m_4, m_1, m_2 and m_3, respectively.

The cross-section for the process is given by

$$\begin{aligned}\sigma = {} & \frac{2SM_1M_2}{\sqrt{s^2-2s(M_1^2+M_2^2)+(M_1^2-M_2^2)^2}} \\ & \times \int \frac{\mathrm{d}^3p_1}{(2\pi)^3}\int \frac{\mathrm{d}^3p_2}{(2\pi)^3}\int \frac{\mathrm{d}^3p_3}{(2\pi)^3}\int \frac{\mathrm{d}^3p_4}{(2\pi)^3}\int \frac{\mathrm{d}^3p_5}{(2\pi)^3} \\ & \times \frac{1}{2\omega_1}\frac{1}{2\omega_2}\frac{m_3}{\omega_3}\frac{1}{2\omega_4}\frac{m_5}{\omega_5} \\ & \times (2\pi)^4\delta^4(q_1+q_2-\sum p_i)|Amp|^2, \end{aligned} \qquad \text{(A.2)}$$

where $S=1/2$ for the symmetry of $\pi^0\pi^0$ and $p_i^\mu = (\omega_i, \mathbf{p}_i)$.

The evaluation of the δ-function of energy conservation for so many particles can be a difficult task. However, it can be extremely simplified by using the following procedure.

The quantity

$$\begin{aligned} A \equiv {} & \int \frac{\mathrm{d}^3p_4}{(2\pi)^3}\int \frac{\mathrm{d}^3p_3}{(2\pi)^3}\frac{1}{\omega_3\omega_4} \\ & \times (2\pi)^4\delta^4(q_1+q_2-\sum p_i)|Amp|^2 \\ = {} & \int \frac{\mathrm{d}^3p_4}{(2\pi)^3}\frac{1}{\omega_3\omega_4} \\ & \times (2\pi)\delta(q_1^0+q_2^0-\sum \omega_i)|Amp|^2 \end{aligned} \qquad \text{(A.3)}$$

is Lorentz invariant, hence we can evaluate it in any desired frame. By convenience we choose a frame where $\mathbf{p}_3+\mathbf{p}_4=0$. In this frame the δ-function of energy conservation is simple since $M_{34}^2=(p_3+p_4)^2=(q_1+q_2-p_1-p_2-p_5)^2=(q_1^0+q_2^0-p_1^0-p_2^0-p_5^0)^2$ and hence $\delta(q_1^0+q_2^0-p_1^0-p_2^0-\omega_3-\omega_4-p_5^0)=\delta(M_{34}-\sqrt{p_4^2+m_3^2}-\sqrt{p_4^2+m_4^2})$ is only a function of $|\mathbf{p}_4|$ and hence can be used to evaluate the $|\mathbf{p}_4|$ integral, which gives

$$A = \int \mathrm{d}\cos\theta_4'\mathrm{d}\phi_4'|\mathbf{p}_4'|\frac{1}{(2\pi)^2}\frac{|\mathbf{p}_4'|}{M_{34}}|Amp|^2\Theta(M_{34}-m_3-m_4), \qquad \text{(A.4)}$$

where $|\mathbf{p}_4'| = \lambda^{1/2}(M_{34}^2, m_3^2, m_4^2)/2M_{34}$ is the momentum in the $\mathbf{p}_3+\mathbf{p}_4=0$ frame.

The final expression for the cross-section is

$$\begin{aligned}\sigma = {} & \frac{SM_1M_2m_3m_5}{4(2\pi)^{11}\sqrt{s^2-2s(M_1^2+M_2^2)+(M_1^2-M_2^2)^2}} \\ & \times \int \mathrm{d}^3p_1\int \mathrm{d}^3p_2\int \mathrm{d}^3p_5\int \mathrm{d}\cos\theta_4'\int \mathrm{d}\phi_4' \\ & \times \frac{|\mathbf{p}_4'|}{\omega_1\omega_2\omega_5M_{34}}\Theta(M_{34}-m_3-m_4)|Amp|^2. \end{aligned} \qquad \text{(A.5)}$$

When evaluating the amplitude all the momenta have to be evaluated in the overall CM frame, hence one has to boost back the $\mathbf{p}_4'$ momentum to this system with the following expression:

$$\mathbf{p}_4 = \mathbf{p}_4' + \left[\left(\frac{P^0}{M_{34}}-1\right)\frac{\mathbf{p}_4'\cdot\mathbf{P}}{|\mathbf{P}|^2}+\frac{p_4'^0}{M_{34}}\right]\mathbf{P}. \qquad \text{(A.6)}$$

with $\mathbf{P}=-\mathbf{p}_1-\mathbf{p}_2-\mathbf{p}_5$ and $P^0=\sqrt{s}-p_1^0-p_2^0-p_5^0$.

The four-body phase space for the

$$p(q_1)p(q_2) \to p(p_2)K^+(p_4)K^-(p_3)p(p_1) \qquad \text{(A.7)}$$

reaction can be evaluated in an analogous way to the previous one and gives

$$\begin{aligned}\sigma = {} & \frac{SM_1M_2m_1m_2}{2(2\pi)^8\sqrt{s^2-2s(M_1^2+M_2^2)+(M_1^2-M_2^2)^2}} \\ & \times \int \mathrm{d}^3p_1\int \mathrm{d}^3p_2\int \mathrm{d}\cos\theta_4'\int \mathrm{d}\phi_4'\frac{|\mathbf{p}_4'|}{\omega_1\omega_2M_{34}} \\ & \times \Theta(M_{34}-m_3-m_4)|Amp|^2, \end{aligned} \qquad \text{(A.8)}$$

where $S=1/2$ since the final protons are identical particles. The boost of p_4' to the overall CM frame is done with eq. (A.6) but now $\mathbf{P}=-\mathbf{p}_1-\mathbf{p}_2$ and $P^0=\sqrt{s}-p_1^0-p_2^0$.

Appendix B. Alternative derivation of the amplitudes

Here we explain in detail the analytic evaluation of the amplitudes for the $pp\to pK^+\pi^0\pi^0\Lambda$ and $pp\to pK^+K^-p$ reactions within the method of irreducible tensors, which is more familiar to many readers than the technique described in the main text.

Let us start by determining the allowed quantum numbers of the initial and final states, which are independent of the internal mechanisms, which will be of help in simplifying the evaluation of the amplitudes later on. Let us consider the general process $pp\to K^+p\Lambda(1520)$. Since the reaction is calculated at energies close to threshold, the only final total angular momentum allowed is $L = 0$. Hence the final J^P possibilities are 1^+ or 2^+, since $J^P(K^+) = 0^-$, $J^P(p) = 1/2^+$ and $J^P(\Lambda(1520)) = 3/2^-$. The spin of the initial pp pair can be 0 or 1 while L has to be even for parity reasons. But, since the initial protons are identical fermions, $L+S+I$ has to be odd. And, since, $I = 1$, then $L+S$ has to be even. Hence the only possibility to match final 1^+ or 2^+ is that the initial protons are in $L = 2$ and $S = 0$. In summary, the initial pp state has the following quantum numbers: $L = 2$, $S = 0$, $P = +$, independent of the internal dynamics and the $\Lambda(1520)$ decay products.

Let us consider now the quantum numbers of the $p\Lambda$ system in the $pp \to pK^+(\Lambda(1520)) \to pK^+(\pi^0\Sigma^*) \to pK^+(\pi^0\pi^0\Lambda)$ reaction. Considering the parity of the final particles and the fact that the $\Lambda(1520)$ decay into $\pi\Sigma^*$ is in s-wave and the decay of the Σ^* into $\pi\Lambda$ is in p-wave, the angular momentum of the $p\Lambda$ system has to be even to match the global parity $+$. Given the typical momenta of the final Λ at the energies of concern in the present work, the only possibility is $L(p\Lambda) = 0$. On the other hand, the spin of the $p\Lambda$ system has to be $S(p\Lambda) = 1$ in order to give total $J = 2$ when combined to the p-wave of the $\Sigma^* \to \pi\Lambda$ decay in line with the formalism as described in the main text.

Regarding the $pp \to pK^+(\Lambda(1520)) \to pK^+(K^-p)$ reaction, the kinematics of the pp final state is that the proton coming from the $\Lambda(1520)$ decay has about $240\,\mathrm{MeV}/c$ momenta since the $\Lambda(1520)$ is produced essentially at rest, and the other proton is also basically at rest in the total CM frame. This gives the protons a kinetic energy of about $8\,\mathrm{MeV}$ in their CM frame where only relative S-waves are relevant. Hence, the final pp system only can be in $L(pp) = 0$ at the energies considered. On the other hand, the spin is $S(pp) = 0$ since $L+S+I$ has to be odd.

Let us evaluate the amplitude for the $pp \to pK^+\pi^0\pi^0\Lambda$ reaction of fig. 2. The amplitude for the vertex pK^+K^-p is given by [2]

$$-it = -i\frac{1}{2f^2}(p_4^0 - k^0). \tag{B.1}$$

The unitarized $\bar{K}N \to \pi\Sigma^*$ transition has the following form [20]:

$$\begin{aligned}-it_{K^-p\to\pi^0\Sigma^{*0}} = -i\frac{1}{\sqrt{2}}\frac{(-1)}{\sqrt{3}}T_{\bar{K}N\to\pi\Sigma^*}&\\ \times\mathcal{C}\left(\frac{1}{2}\ 2\ \frac{3}{2};-m,M+m\right)&\\ \times Y_{2,-m-M}(\hat{k})(-1)^{M+m}\sqrt{4\pi}\,,&\end{aligned} \tag{B.2}$$

where $\mathcal{C}$ are Clebsch-Gordan coefficients. For the decay of the Σ^* into $\pi^0\Lambda$, the vertex is [36]

$$-it = -\frac{f_{\Sigma^*\pi\Lambda}}{m_\pi}\left\langle\frac{1}{2}m''|\mathbf{S}\cdot\mathbf{p}_2|\frac{3}{2}M\right\rangle, \tag{B.3}$$

where $f_{\Sigma^*\pi\Lambda}/m_\pi = 9.61\times10^{-3}\,\mathrm{MeV}^{-1}$ and $\mathbf{S}$ is the total spin 3/2 to 1/2 transition operator given by:

$$\mathbf{S}\cdot\mathbf{p} = \begin{pmatrix} -\frac{p_x+ip_y}{\sqrt{2}} & \sqrt{\frac{2}{3}}p_z & \frac{p_x-ip_y}{\sqrt{6}} & 0\\ 0 & -\frac{p_x+ip_y}{\sqrt{6}} & \sqrt{\frac{2}{3}}p_z & \frac{p_x-ip_y}{\sqrt{2}}\end{pmatrix}. \tag{B.4}$$

Hence, the full amplitude is given by

$$\begin{aligned}t={}&i\frac{1}{2f^2}(p_4^0-k^0)\frac{1}{k^2-m_K^2}\frac{1}{\sqrt{s_{\Sigma^*}}-M_{\Sigma^*}+i\Gamma_{\Sigma^*}(\sqrt{s_{\Sigma^*}})/2}\\ &\times\frac{f_{\Sigma^*\pi\Lambda}}{m_\pi}\frac{1}{\sqrt{6}}T_{\bar{K}N\to\pi\Sigma^*}\ \mathcal{C}\left(\frac{1}{2}\ 2\ \frac{3}{2};-m,M+m\right)\\ &\times Y_{2,-m-M}(\hat{k})(-1)^{M+m}\sqrt{4\pi}\left\langle\frac{1}{2}m''|\mathbf{S}\cdot\mathbf{p}_2|\frac{3}{2}M\right\rangle\\ &\times\delta_{m',m}\delta_{M,-m},\end{aligned} \tag{B.5}$$

where $s_{\Sigma^*} = (p_2+p_3)^2$.

Since the momentum of the exchanged kaon is approximately equal to the incoming proton momentum, we can do the following approximation:

$$Y_{2,-m-M}(\hat{k}) \simeq Y_{2,-m-M}(\hat{u_z}) = \sqrt{\frac{5}{4\pi}}\,. \tag{B.6}$$

On the other hand, the spin of the initial pp system is $S(pp) = 0$ (antisymmetric) and the spin of the final $p\Lambda$ system is $S(p\Lambda) = 1$ (symmetric), as discussed above. Therefore, the initial spin wave function has to be antisymmetrized and the final $p\Lambda$ spin wave function has to be symmetrized. Let us consider only the spin-dependent part of eq. (B.5). The antisymmetrization of the initial spin gives

$$\begin{aligned}&\frac{1}{\sqrt{2}}\left[\mathcal{C}\left(\frac{1}{2}\ 2\ \frac{3}{2};-\frac{1}{2}\ 0\right)\left\langle\frac{1}{2}m''|\mathbf{S}\cdot\mathbf{p}_2|\frac{3}{2}-\frac{1}{2}\right\rangle\delta_{m',+1/2}\right.\\ &\qquad\left.-\,\mathcal{C}\left(\frac{1}{2}\ 2\ \frac{3}{2};+\frac{1}{2}\ 0\right)\left\langle\frac{1}{2}m''|\mathbf{S}\cdot\mathbf{p}_2|\frac{3}{2}+\frac{1}{2}\right\rangle\delta_{m',-1/2}\right]\\ &=\frac{1}{\sqrt{2}}\sqrt{\frac{2}{5}}\left[\left\langle\frac{1}{2}m''|\mathbf{S}\cdot\mathbf{p}_2|\frac{3}{2}-\frac{1}{2}\right\rangle\delta_{m',+1/2}\right.\\ &\qquad\left.+\left\langle\frac{1}{2}m''|\mathbf{S}\cdot\mathbf{p}_2|\frac{3}{2}+\frac{1}{2}\right\rangle\delta_{m',-1/2}\right].\end{aligned} \tag{B.7}$$

Now we have to symmetrize the latter expression for the final $p\Lambda$ spin. For $S_z(p\Lambda) = 0$ it gives

$$\begin{aligned}&\frac{1}{\sqrt{2}}\frac{1}{\sqrt{2}}\sqrt{\frac{2}{5}}\left[\left\langle\frac{1}{2}-\frac{1}{2}|\mathbf{S}\cdot\mathbf{p}_2|\frac{3}{2}-\frac{1}{2}\right\rangle+0\right.\\ &\qquad\left.+\,0+\left\langle\frac{1}{2}+\frac{1}{2}|\mathbf{S}\cdot\mathbf{p}_2|\frac{3}{2}+\frac{1}{2}\right\rangle\right]\\ &=\sqrt{\frac{2}{5}}\sqrt{\frac{2}{3}}p_{2z},\end{aligned} \tag{B.8}$$

for $S_z(p\Lambda) = -1$:

$$\frac{1}{\sqrt{2}}\sqrt{\frac{2}{5}}\left[0+\left\langle\frac{1}{2}-\frac{1}{2}|\mathbf{S}\cdot\mathbf{p}_2|\frac{3}{2}+\frac{1}{2}\right\rangle\right]$$
$$= -\frac{1}{\sqrt{5}}\frac{1}{\sqrt{6}}(p_{2x}+ip_{2y}), \qquad \text{(B.9)}$$

and for $S_z(p\Lambda) = +1$:

$$\frac{1}{\sqrt{2}}\sqrt{\frac{2}{5}}\left[\left\langle\frac{1}{2}+\frac{1}{2}|\mathbf{S}\cdot\mathbf{p}_2|\frac{3}{2}-\frac{1}{2}\right\rangle+0\right]$$
$$= \frac{1}{\sqrt{5}}\frac{1}{\sqrt{6}}(p_{2x}-ip_{2y}). \qquad \text{(B.10)}$$

Hence, the final expression for the amplitude is

$$t = -i\frac{1}{3}\frac{1}{2f^2}(p_4^0-k^0)\frac{1}{k^2-m_k^2}$$
$$\times\frac{1}{\sqrt{s_{\Sigma^*}}-M_{\Sigma^*}+i\Gamma_{\Sigma^*}(\sqrt{s_{\Sigma^*}})/2}\frac{f_{\Sigma^*\pi\Lambda}}{m_\pi}$$
$$\times T_{\bar{K}N\to\pi\Sigma^*}\left\{\begin{array}{ll}\sqrt{2}p'_{2z} & S_z=0\\ \frac{1}{2}(p'_{2x}-ip'_{2y}) & S_z=+1\\ -\frac{1}{2}(p'_{2x}+ip'_{2y}) & S_z=-1\end{array}\right\} \qquad \text{(B.11)}$$

and the symmetrization of the identical pions has to be considered by adding, for each S_z, the amplitude changing $p_1 \leftrightarrow p_2$.

For the evaluation of the $pp \to pK^+K^-p$ amplitude we need the unitarized $K^-p \to K^-p$ amplitude which is given by

$$-it_{K^-p\to K^-p} = -i\frac{1}{2}T_{\bar{K}N\to\bar{K}N}\sum_M \mathcal{C}\left(\frac{1}{2}\ 2\ \frac{3}{2};-m,M+m\right)$$
$$\times Y_{2,-m-M}(\hat{k})\mathcal{C}\left(\frac{1}{2}\ 2\ \frac{3}{2};m'',M-m''\right)$$
$$\times Y^*_{2,m''-M}(\hat{p_3})(-1)^{m''+m}4\pi. \qquad \text{(B.12)}$$

The rest of the procedure is analogous to the previous case but now the final pp spin is $S(pp)=0$, as discussed above, which is antisymmetric and hence we have now to antisymmetrize the final pp spin wave function.

The final expression of the amplitude is given by

$$t(p_1,p_2) = \frac{1}{2f^2}(p_4^0-k^0)\frac{1}{k^2-m_k^2}\frac{1}{2}(3\cos^2\theta_3-1)T_{\bar{K}N\to\bar{K}N}, \qquad \text{(B.13)}$$

where the symmetry of the final pp space wave function has to be considered by adding to the amplitude the same expression changing $p_1 \leftrightarrow p_2$.

References

1. N. Kaiser, T. Waas, W. Weise, Nucl. Phys. A **612**, 297 (1997).
2. E. Oset, A. Ramos, Nucl. Phys. A **635**, 99 (1998).
3. U.-G. Meißner, J.A. Oller, Nucl. Phys. A **673**, 311 (2000) [arXiv:nucl-th/9912026].
4. J.A. Oller, U.-G. Meißner, Phys. Lett. B **500**, 263 (2001).
5. C. Garcia-Recio, J. Nieves, E. Ruiz Arriola, M.J. Vicente Vacas, Phys. Rev. D **67**, 076009 (2003).
6. T. Hyodo, A. Hosaka, E. Oset, A. Ramos, M.J. Vicente Vacas, Phys. Rev. C **68**, 065203 (2003).
7. J.A. Oller, E. Oset, A. Ramos, Prog. Part. Nucl. Phys. **45**, 157 (2000).
8. D. Jido, J.A. Oller, E. Oset, A. Ramos, U.-G. Meißner, Nucl. Phys. A **725**, 181 (2003).
9. C. Garcia-Recio, M.F.M. Lutz, J. Nieves, Phys. Lett. B **582**, 49 (2004).
10. Crystall Ball Collaboration (S. Prakhov *et al.*), Phys. Rev. C **70**, 034605 (2004).
11. D.W. Thomas, A. Engler, H.E. Fisk, R.W. Kraemer, Nucl. Phys. B **56**, 15 (1973).
12. V.K. Magas, E. Oset, A. Ramos, Phys. Rev. Lett. **95**, 052301 (2005).
13. E.E. Kolomeitsev, M.F.M. Lutz, Phys. Lett. B **585**, 243 (2004).
14. S. Sarkar, E. Oset, M.J. Vicente Vacas, Nucl. Phys. A **750**, 294 (2005).
15. T. Nakano, talk at the *Pentaquark04 meeting*, `http://www.rcnp.osaka-u.ac.jp/~ penta04/`.
16. K.H. Hicks, Prog. Part. Nucl. Phys. **55**, 647 (2005).
17. Particle Data Group (S. Eidelman *et al.*), Phys. Lett. B **592**, 1 (2004).
18. T.S. Mast, M. Alston-Garnjost, R.O. Bangerter, A. Barbaro-Galtieri, F.T. Solmitz, R.D. Tripp, Phys. Rev. D **7**, 5 (1973).
19. S. Prakhov *et al.*, Phys. Rev. C **69**, 042202 (2004).
20. S. Sarkar, E. Oset, M.J. Vicente Vacas, Phys. Rev. C **72**, 015206 (2005).
21. L. Roca, S. Sarkar, V.K. Magas, E. Oset, Phys. Rev. C **73**, 045208 (2006); S. Sarkar, L. Roca, E. Oset, V.K. Magas, M.J.V. Vacas, arXiv:nucl-th/0511062.
22. J.A. Oller, E. Oset, Phys. Rev. D **60**, 074023 (1999).
23. E. Jenkins, A.V. Manohar, Phys. Lett. B **259**, 353 (1991).
24. R. Maier, private communication.
25. I. Zychor *et al.*, Phys. Rev. Lett. **96**, 012002 (2006); P. Winter *et al.*, Phys. Lett. B **635**, 23 (2006).
26. C. Hanhart, Phys. Rep. **397**, 155 (2004).
27. A. Gasparyan, J. Haidenbauer, C. Hanhart, Phys. Rev. C **72**, 034006 (2005).
28. A. Sibirtsev, J. Haidenbauer, H.W. Hammer, S. Krewald, arXiv:nucl-th/0512059.
29. F. Hinterberger, A. Sibirtsev, Eur. Phys. J. A **21**, 313 (2004).
30. M.A. Preston, R.K. Bhaduri, *Structure of the Nucleus* (Addison Wesley, 1975) pp. 39-51.
31. A. Sibirtsev, W. Cassing, Eur. Phys. J. A **7**, 407 (2000).
32. B.L. Druzhinin, A.E. Kudryavtsev, V.E. Tarasov, Z. Phys. A **359**, 205 (1997).
33. C. Hanhart, K. Nakayama, Phys. Lett. B **454**, 176 (1999).
34. S. Weinberg, Phys. Rev. **130**, 776 (1963).
35. V. Baru *et al.*, Phys. Lett. B **586**, 53 (2004) [arXiv:hep-ph/0308129].
36. E. Oset, A. Ramos, Nucl. Phys. A **679**, 616 (2001).